THE ASTRONOMICAL JOURNAL, 120:2687–2694, 2000 November

A WIDE-FIELD CCD SURVEY FOR CENTAURS AND KUIPER BELT OBJECTS

SCOTT S. SHEPPARD, DAVID C. JEWITT, AND CHADWICK A. TRUJILLO
Institute for Astronomy, University of Hawaii, 2680 Woodlawn Drive, Honolulu, HI 96822; sheppard@ifa.hawaii.edu, jewitt@ifa.hawaii.edu, chad@ifa.hawaii.edu

MICHAEL J. I. BROWN
School of Physics, University of Melbourne, Parkville, VIC 3010, Australia; mbrown@isis.ph.unimelb.edu.au

AND

MICHAEL C. B. ASHLEY
School of Physics, University of New South Wales, NSW 2052, Australia; mcba@newt.phys.unsw.edu.au
Received 2000 April 10; accepted 2000 July 31

ABSTRACT

A modified Baker-Nunn camera was used to conduct a wide-field survey of 1428 deg^2 of sky near the ecliptic in search of bright Kuiper Belt objects and Centaurs. This area is an order of magnitude larger than any previously published CCD survey for Centaurs and Kuiper Belt objects. No new objects brighter than red magnitude $m_R = 18.8$ and moving at a rate 1″ to 20″ hr^{-1} were discovered, although one previously discovered Centaur, 1997 CU_{26} (Chariklo), was serendipitously detected. The parameters of the survey were characterized using both visual and automated techniques. From this survey, the empirical projected surface density of Centaurs was found to be $\Sigma_C(m_R \leq 18.8) = 7.8^{+16.0}_{-6.6} \times 10^{-4}$ deg^{-2}, and we found a projected surface density 3 σ upper confidence limit for Kuiper Belt objects of $\Sigma_K(m_R \leq 18.8) < 4.1 \times 10^{-3}$ deg^{-2}. We discuss the current state of the cumulative luminosity functions of both Centaurs and Kuiper Belt objects. Through a Monte Carlo simulation we show that the size distribution of Centaurs is consistent with a $q \sim 4$ differential power law, similar to the size distribution of the parent Kuiper Belt objects. The Centaur population is of order 1×10^7 (radius ≥ 1 km), assuming a geometric albedo of 0.04. We predict about 100 Centaurs larger than 50 km in radius, of which only four are presently known. The current total mass of the Centaurs is about 10^{-4} $M_\oplus$. No dust clouds were detected resulting from Kuiper Belt object collisions, placing a 3 σ upper limit of fewer than 600 collisionally produced clouds of $m_R < 18.8$ per year.

Key words: Kuiper belt, Oort cloud — minor planets, asteroids — solar system: general — surveys

1. INTRODUCTION

The outer solar system has recently been found to be populated by a vast number of minor bodies (see, e.g., Jewitt, Luu, & Chen 1996; Jedicke & Herron 1997; Jewitt, Luu, & Trujillo 1998). As of 2000 June there are 20 objects, known as Centaurs, that have semimajor axes and perihelia between Jupiter and Neptune and over 300 objects, known as Kuiper Belt objects (KBOs), that have semimajor axes greater than that of Neptune. Centaurs are believed to have originated from the Kuiper Belt and are now in dynamically unstable orbits that will lead either to ejection from the solar system, an impact with a planet or the Sun, or evolution into a short-period comet. The brightest known KBO, other than Pluto-Charon, has apparent red magnitude $m_R \sim 20$, whereas several Centaurs are brighter than this. With current technology, physical and chemical properties of only the largest and brightest minor bodies in the outer solar system can be studied. Centaurs and KBOs could be the most primitive bodies in the solar system, and they represent a unique opportunity to probe the early history of the local solar nebula.

The cumulative luminosity function (CLF) describes the sky-plane surface density of objects brighter than a given magnitude. Little work has been done on the CLF of Centaurs (Jewitt et al. 1996; Levison & Duncan 1997), but the CLF of KBOs is well defined for magnitudes $20 \lesssim m_R \lesssim 26$ (Gladman et al. 1998; Jewitt et al. 1998; Luu & Jewitt 1998; Chiang & Brown 1999). The bright end of the KBO CLF is very uncertain because bright KBOs are rare and a limited amount of sky has been searched. The extrapolated CLF currently predicts about one KBO of $m_R \leq 19$ per 500 square degrees of sky. Observations with possible bearing on large bodies in the outer solar system include the high eccentricities and inclinations of KBOs, which could have come from massive planetesimals in the outer solar system (Morbidelli & Valsecchi 1997), and the obliquity of Uranus's spin axis, which might imply a collision with a massive body (Singer 1975). Models of the evolution of the outer solar system suggest that a more massive disk was needed in the primordial Kuiper Belt to explain its current population size structure (Stern 1996b). A detailed accretion model of the early Kuiper Belt by Kenyon & Luu (1999) has shown that several Pluto-sized objects could form within the age of the solar system. Direct evidence for large objects in the outer solar system includes the large irregular satellite Triton, as well as the Pluto-Charon system. To constrain the CLF of both the Centaurs and the KBOs at $m_R \leq 20$ requires searches covering large sky areas. To date, large surveys have been conducted using photographic plates, which are difficult to parameterize. A list of surveys that have covered over 50 deg^2 and had temporal sampling sufficient to detect Centaurs, KBOs, or both is given in Table 1. Considering that relatively little of the sky has been searched for these slow-moving objects (SMOs), and that recent advances in CCD technology have made large-area surveys feasible, this is an excellent time to search for bright SMOs. Accordingly, we undertook a wide-field survey in search of bright objects in the outer solar system.

TABLE 1

LARGE AND MEDIUM-SIZED SEARCHES FOR SLOW-MOVING OBJECTS

SURVEY	SQUARE DEGREES[b]		LIMITING MAGNITUDE	DETECTED OBJECTS[c]		OBJECTS[d]	YEARS
	KBOs	Centaurs	(m_R)	KBOs	Centaurs	(m_R)	
Tombaugh 1961[e]	1530	1530	16.8	0	0	...	1939–1940
	~19500	~19500	15.5	1	0	14	1929–1945
	~25500	~25500	15		0		
	~28000	~28000	13		0		
Kowal 1989[e]	6400	6400	19.5	0	1	18	1976–1985
This work	1428	1428	18.8	0	0 (1)	...	1999
Luu & Jewitt 1988[e].....	297	297	19.5[f]	0	0	...	1987
Jewitt et al. 1998.....	51.5	51.5	22.5	13	0	20.60	1996–1997
Irwin, Tremaine, & Żytkow 1995[e]	50	50	20	0	0	...	1995
Spacewatch.....	~1000	~10000	20–21[f]	7	8 (1)	16.5, 17.4,[f] 19.5, 20.4[f]	1989–
LONEOS.....	0	?[g]	~19	...	0 (2)	...	1998–
Catalina.....	0	?[h]	~19	...	1 (1)	18	1999–

NOTE.—For searches that cover over 50 deg^2. Spacewatch, LONEOS, and Catalina are near-Earth object searches capable of detecting some SMOs. Data for these programs are from R. McMillan (1999, private communication), B. Koehn (1999, private communication), and S. Larson (1999, private communication), respectively.

[b] Area covered in which KBOs ($d\theta/dt < 4''$ hr^{-1}) and Centaurs ($4''$ hr$^{-1} < d\theta/dt < 20''$ hr^{-1}) could be detected.

[c] Number of new objects detected, as well as serendipitously detected known objects (in parentheses).

[d] The magnitude of the brightest object(s) detected in the survey.

[e] Performed using photographic plates.

[f] Calculated from quoted V-band value using $V-R=0.5$.

[g] Covers most of the sky north of $-30°$ declination.

[h] Covers about 300 deg^2 per good night.

2. OBSERVATIONS

The 0.5 m diameter Automated Patrol Telescope (APT) at Siding Spring Observatory, in Australia, was used during three observing runs in early 1999. The APT is a modified Baker-Nunn camera using a three-element lens to achieve a corrected wide field of view (Carter et al. 1992). It was originally designed to track satellites in Earth orbit. We used a 770 × 1152 pixel CCD manufactured by EEV with 22.5 μm pixels and a pixel scale of $9''.41$ pixel^{-1} at the f/1 focal plane for imaging. The quantum efficiency of the detector is 0.46 in the R band. The detector has a 3° × 2° rectangular field of view, with the east-west direction aligned parallel to the long axis. Exposures were taken using a Johnson R-band filter, and the telescope was tracked at sidereal rate. The APT site is exceptionally dark. The seeing was usually around $1''.5$ as measured from other telescopes on the mountain. At the APT, the large pixel scale did not allow us to directly measure the seeing, and moderate variations in seeing were not noticeable. The data were undersampled, which made it difficult to distinguish between galaxies and stars (see Fig. 1).

A total of 238 independent fields covering 1428 deg^2 of sky were imaged during observing runs centered around new Moon in 1999 January, February, and March (Table 2). A map of the sky areas searched is shown in Figure 2, and the specific field centers are given in Table 3. The fields were selected to be observed at an air mass ≤ 1.5 and to be within 30° of the ecliptic. Selection of the fields was made with no prior knowledge of known SMOs in the area. The search was made between +10° and −30° of the ecliptic. The observational strategy was to search within ±1.5 hr of opposition. At opposition, the movement of an object is simply related to heliocentric distance by

$$\frac{d\theta}{dt} \approx \frac{148}{R + R^{1/2}}, \quad (1)$$

where R (AU) is the heliocentric distance and $d\theta/dt$ (arcsec hr^{-1}) is the rate of change of apparent position of the SMO

TABLE 2

APT SURVEY DATA

Date	Nights	Images	Fields	Sky Area (deg^2)
1999 Jan.....	10	201	58	348
1999 Feb	15	468	112	672
1999 Mar.....	15	399	68	408
Total	40	1068	238	1428

TABLE 3

OBSERVATIONS FROM THE AUTOMATED PATROL TELESCOPE

Field	R.A. (J2000.0)	Decl. (J2000.0)	UT Date
f0991.....	07 29 24	16 00 00	1999 Jan 13, 14, 15
f0044.....	08 35 60	00 00 00	1999 Jan 15, 17, 18
f3926.....	08 53 11	−08 00 00	1999 Feb 17, 19, 21
f0409.....	09 27 06	06 00 00	1999 Feb 14, 15, 16
f1003.....	09 59 12	16 00 00	1999 Feb 16, 17, 18
f4288.....	10 18 22	−14 00 00	1999 Feb 13, 14, 15
f3933.....	10 18 00	−08 00 00	1999 Mar 11, 12, 14
f3703.....	12 13 47	−04 00 00	1999 Mar 20, 22, 23

NOTE.—Centaur Chariklo was found in field f0409. Table 3 is presented in its entirety in the electronic edition of the Astronomical Journal. A portion is shown here for guidance regarding its form and content.

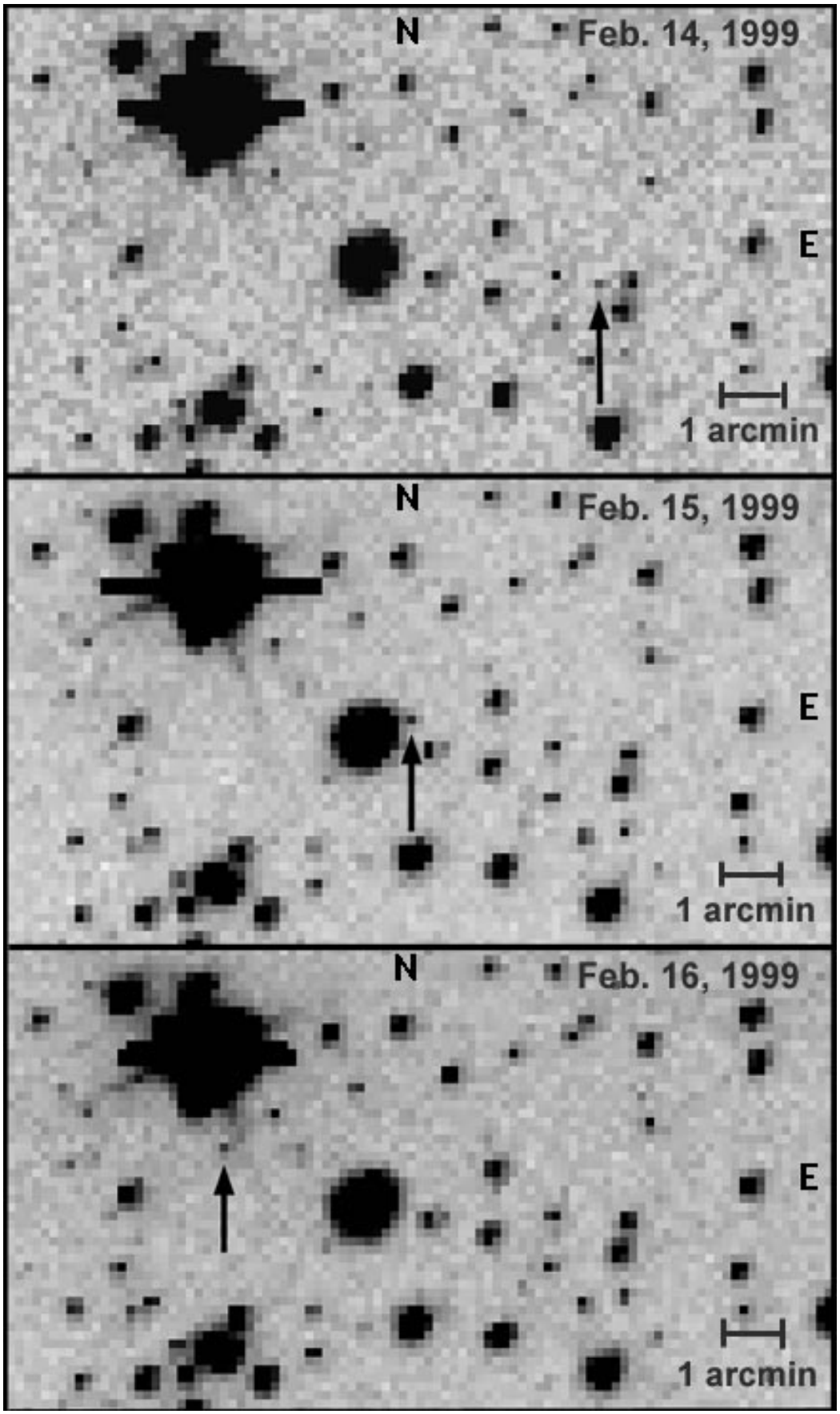

FIG. 1.—Portions of three APT fields collected during the run in 1999 February, with a 1 day time base between images. The width of each image section is $\frac{1}{4}^\circ$, and the height is $\frac{1}{8}^\circ$. Each image section shows 0.5% of the total area of one field. The arrows show the position of the Centaur 1997 CU_{26} (Chariklo) on each night.

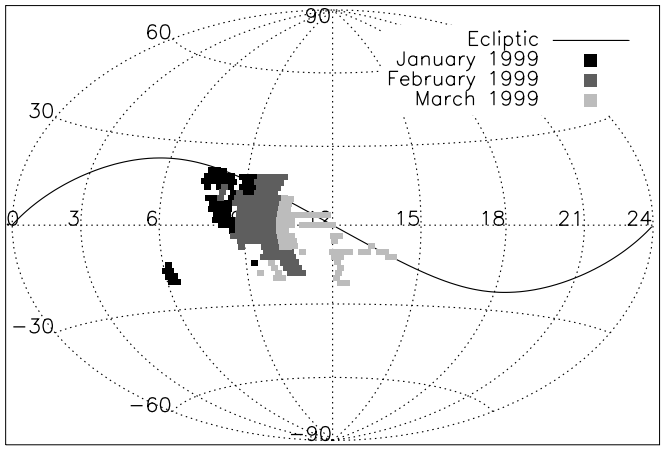

FIG. 2.—Sky covered during this survey. Shaded areas represent the month in which the sky was searched. The horizontal axis is right ascension in hours, and the vertical axis is declination in degrees.

on the CCD. From equation (1), KBOs with $R > 30$ AU will have $d\theta/dt \leq 4''$ hr^{-1} ($\leq$10 pixels per day) and Centaurs with 5 AU $< R <$ 30 AU have $4''$ hr$^{-1} \leq d\theta/dt \leq 20''$ hr^{-1} (between 10 and 50 pixels per day). Therefore, we sought KBOs and Centaurs by comparing images taken on successive nights, allowing the detection of objects moving at rates between $1''$ and $20''$ hr^{-1}. Trailing of both KBOs and Centaurs was negligible because of the large pixels, slow movement of the objects, and short integration times.

Three consecutive exposures of 200 s each were taken on each of three separate nights, yielding nine images per field. Weather permitting, the fields were imaged on consecutive nights. The images were bias- and dark-subtracted and then flat-fielded with median twilight sky flats. The three images of a field taken during a single night were registered and then combined using the IRAF CRREJECT cosmic-ray rejection algorithm to remove cosmic rays and increase signal-to-noise ratio. These three images were taken consecutively, so there was little or no telescope motion between them. Landolt (1992) standard stars were used for photometric calibration.

Field centers differed by up to $50''$ from night to night as a result of APT pointing variations. We aligned the fields from different nights by eye. The data were analyzed in two complementary ways, (1) by visual "blinking" and (2) using an automated search algorithm. For the visual analysis, four criteria were used for SMO identification: (*a*) the object must appear in all three frames, (*b*) it must have linear motion, (*c*) it must have a steady brightness in all three frames, and (*d*) it must have constant velocity appropriate for an SMO ($<20''$ hr^{-1}). Many asteroids between magnitudes 10 and 19 were quickly identified and rejected by their large motions ($>$50 pixels in 24 hr). They were not followed up with further observations, because of limited telescope time. Centaur 10199 Chariklo (provisional designation 1997 CU_{26}) was at $m_V = 17.8$ when detected serendipitously (Fig. 1). It was discovered independently by the visual and automated procedures, with no knowledge of its location in the field. No other known SMOs in the area searched were bright enough to be detected by our survey. It should also be noted that the January fields were crowded because of the close proximity of the Galactic plane to opposition, while the March fields were hampered by bad weather. During poor weather, the few fields with gaps of 2 or 3 days were observed on four nights instead of the usual three to ensure that SMO identification efficiency was not significantly reduced compared with fields taken on three consecutive nights.

The limiting magnitude of the survey was found by randomly placing 100 artificial SMOs onto a subset of the images. A Moffat (1969) profile matched to the point-spread function of the APT was used to generate the artificial SMOs. The visual detection efficiencies for KBOs and Centaurs are shown as a function of magnitude in Table 4. A KBO detection efficiency equal to half the maximum efficiency was reached at $m_R = 18.8$, which we take as the limiting magnitude of this survey. The Centaur detection efficiency equal to half the maximum efficiency was also reached near $m_R = 18.8$.

As a complement to the visual SMO search, a moving-object detection program was used to flag potential SMO candidates for scrutiny. The algorithm was optimized for our undersampled data. Objects were detected in each image by searching for maxima in the center of a 3×3 pixel box. An approximate signal-to-noise ratio and flux for the object were then determined using all pixels within the box with flux more than 1.5 σ above the sky background. While this underestimated the flux of extended objects, it provided a good estimate of the flux of faint undersampled stellar images, which occupied 1 to 4 pixels, depending on the location of the image centroid with respect to the pixel grid. Using catalogs of objects in each field with signal-to-noise ratio greater than 4, the software removed stationary objects by searching for objects within ± 1 pixel of the same position in multiple images. Stationary objects with fluxes that varied by more than a factor of 2 are retained in the catalog, as these could be blended objects. The program then flags "objects" with a consistent rate of motion between $1''$ and $12''$ hr^{-1} within 20° of the projected direction of the ecliptic. Candidates with fluxes varying by more than a factor of 5 were rejected, as these were dominated by spurious objects and variable stars.

The software successfully detected Centaur Chariklo, which was not unexpected, as it was more than a magnitude brighter than the survey limit. As with searching for candidates by eye, the detection efficiency was determined by searching for artificial SMOs. The average detection efficiency as a function of magnitude is summarized in Table 5. The KBO detection rate of half the maximum value was reached at $m_R = 18.5$ and is the limiting magnitude for the

TABLE 4

EYE DETECTION EFFICIENCY VERSUS MAGNITUDE FOR ARTIFICIAL KBOS AND CENTAURS

Magnitude (m_R)	KBOs[a] (%)	Centaurs[b] (%)
18.00	92	90
18.25	90	86
18.50	77	72
18.75	55	47
19.00	16	7

[a] Artificial KBOs moved between 8 and 10 pixels day^{-1} ($3''$ to $4''$ hr^{-1}).

[b] Artificial Centaurs moved between 15 and 30 pixels day^{-1} ($6''$ to $12''$ hr^{-1}).

TABLE 5

AUTOMATED DETECTION EFFICIENCY VERSUS MAGNITUDE FOR ARTIFICIAL KBOs AND CENTAURS

Magnitude (m_R)	SMO[a] (%)
17.00	74
17.25	68
17.50	67
17.75	58
18.00	54
18.25	44
18.50	41
18.75	21
19.00	6

[a] Artificial slow-moving objects moved between 3″ and 8″ hr^{-1}.

automated detection technique. The code is not as effective as the eye at deblending merged objects, so the ~50% magnitude limit is ~0.3 mag brighter than that determined by eye. However, in high Galactic latitude fields the efficiency of the code improved significantly, with ~70% of $m_R <$ 18.5 KBOs being detected.

3. RESULTS AND DISCUSSION

A total of 238 fields were examined, covering 1428 deg^2 of sky (about 3.5% of the whole sky). No new SMOs were detected. One previously discovered Centaur (Chariklo) was serendipitously detected. From the one detected Centaur and the efficiency of this survey, we found the empirical projected surface density of Centaurs to be

$$\Sigma_C(m_R \leq 18.8) = 7.8^{+16.0}_{-6.6} \times 10^{-4} \text{ deg}^{-2} . \quad (2)$$

Assuming Poisson statistics, the 3 σ upper confidence limit for the projected surface density of KBOs from our survey is

$$\Sigma_K(m_R \leq 18.8) < 4.1 \times 10^{-3} \text{ deg}^{-2} . \quad (3)$$

We plot these and cumulative surface density measurements from other surveys for Centaurs and KBOs in Figures 3 and 5 below, respectively. Error bars were calculated at 1 σ confidence from detection efficiencies and Poisson error statistics when not explicitly given in the published papers (Gehrels 1986). Quoted upper limits are Poisson 3 σ confidence limits. The CLF is modeled by

$$\log \Sigma(m_R) = \alpha(m_R - m_0) , \quad (4)$$

where $\Sigma(m_R)$ is the number of objects per square degree brighter than m_R, m_0 is the magnitude at which $\Sigma = 1$ deg^{-2}, and 10^{α} describes the slope of the luminosity function.

3.1. *Centaurs*

The current state of the CLF of Centaurs is shown in Figure 3. Almost half of the known Centaurs have been found by the Spacewatch program (Jedicke & Herron 1997; R. McMillan 1999, private communication). The parameters of the Spacewatch survey have changed with time as the detector and observing strategy have been modified. R. McMillan, head of the Spacewatch program, kindly provided estimates of the Spacewatch survey parameters (Table 1). Spacewatch points in Figures 3 and 4 were calculated using the total area searched with the number of Centaurs found.

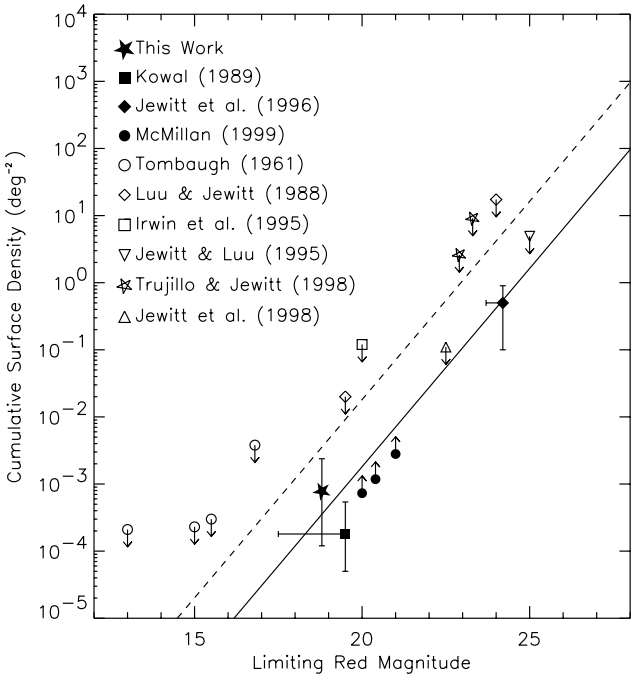

FIG. 3.—Cumulative luminosity function of the Centaurs. Symbols with downward-pointing arrows represent 3 σ upper limits from surveys with null results. Symbols with upward-pointing arrows are lower limits. Others are from published surveys. The dashed line is the fit to the KBO data in Fig. 5; the solid line is the same fit shifted vertically to fit the Centaur CLF.

They are lower limits, since the effective area searched is less than the reported total area searched as a result of some observations in marginal observing conditions and some areas covered multiple times. Kowal's (1989) Centaur constraint is plotted with a sizable uncertainty because of the large trailing losses incurred in long (75 minute) photographic integrations on (relatively) fast-moving Centaurs. The CLF of the Kuiper Belt (see § 3.2) is overplotted on the Centaur data in Figure 3. A line of the same slope has been vertically shifted to run through the points having one or more Centaur detections. The offset line is consistent with every observational point shown in Figure 3, within the uncertainties of measurement. The Centaurs reach $\Sigma = 1$ deg^{-2} at $m_R = 24.6 \pm 0.3$. Thus, Centaurs have an apparent sky-plane density about 10 times less than that of the KBOs at a given magnitude.

The CLF represents the convolved effects of the size and distance distributions of the objects. A Monte Carlo simulation was used to determine the total number of Centaurs larger than a certain radius. The Centaurs were assumed to follow a differential power-law radius distribution of the form $n(r)dr = \Gamma r^{-q} dr$, where Γ and q are constants, r is the radius of the Centaur, and $n(r)dr$ is the number of Centaurs with radii in the range r to $r + dr$. The radii of the Centaurs were assumed to lie between $r_{\min}$ and $r_{\max}$. To find the total number of Centaurs, we adopted $r_{\min} = 1$ km (since the smaller short-period comets are about this size) and $r_{\max} =$ 1000 km (about the size of the largest known trans-Neptunian body, Pluto). The derived total number of Centaurs is insensitive to $r_{\max}$. The surface density distribution of Centaurs in the plane of the ecliptic varies with heliocentric distance and was assumed to be a power law of the form $n(R)dR = \Sigma_0 R^{-\gamma} dR$, where Σ_0 and γ are constants, R is the heliocentric distance, and $n(R)dR$ is the number of

objects with heliocentric distance in the range R to $R + dR$. The heliocentric distance was taken to lie between 10 and 30 AU. A $\gamma = -1.3$ was chosen as the most likely Centaur distance distribution, based on the simulation by Levison & Duncan (1997).

The Monte Carlo simulation was performed by randomly choosing a distance and radius for up to 10^8 Centaurs from the two power-law equations above. Each Centaur's apparent magnitude at opposition was then calculated using

$$m_R = m_\odot - 2.5 \log [p_R r^2 \phi(\alpha)/(2.25 \times 10^{16} R^2 \Delta^2)] , \quad (5)$$

in which r is in kilometers, R is in AU, Δ is the geocentric distance in AU (taken here to be $\Delta = R - 1$), $m_\odot$ is the apparent red magnitude of the Sun (-27.1), m_R is the apparent red magnitude of the Centaur, p_R is the geometric red albedo, assumed to be 0.04, and $\phi(\alpha)$ is the phase function, in which the phase angle $\alpha = 0°$ at opposition and thus $\phi(0) = 1$.

The results of the Monte Carlo simulations using $q = 3.5$, 4.0, and 4.5 are shown in Figure 4. We obtained the total number of Centaurs with $r > 1$ km by normalizing the simulation to the CLF of the Centaurs at $m_R = 22.0$. We assumed that the inclination distribution extends to $\pm 30°$ in latitude from the ecliptic; the total sky area occupied by Centaurs is then about 20,000 deg^2. We used the relation $N(>r) = \Gamma/(q-1) r^{q-1}$, where N is the cumulative number of Centaurs with radius greater than r, to find Γ. Table 6 shows the results for the number of Centaurs using different assumed values of the main parameters. For the $q = 4$ index, we found that there are about 1×10^7 Centaurs with $r > 1$ km. Uncertainties in q of ± 0.5 correspond to uncertainties in the population by factors of 3 to 4. Plausible uncertainties in γ have a smaller effect (see Table 6).

The $q = 3.5$, 4.0, and 4.5 curves are all consistent with the Centaur CLF (Fig. 4). If we use the closest fit, $q = 4$, simulation, we obtain $N(r > 50 \text{ km}) \sim 100$ (Table 6). The number of Centaurs with $r > 50$ km is comparable to the 300 main-belt asteroids (Tedesco 1989) in this size regime but much smaller than the 7×10^4 KBOs expected with $r > 50$ km (Jewitt et al. 1998). Our result is about an order of magnitude smaller than the result obtained by Jewitt et al. (1996). These authors detected two Centaurs in a narrow-field survey and crudely estimated the Centaur population based on only one of the Centaurs and in the absence of a model of the Centaur radial distance distribution. Jedicke & Herron (1997) found, at the 99% confidence level, that there must be fewer than 250 Centaurs with $r > 50$ km (we scaled the quoted value for $r > 25$ km in Jedicke & Herron 1997 to $r > 50$ km using $q = 4$ for the size distribution), and they also concluded there are three or fewer Centaurs with $r > 100$ km. Although all three results are consistent within the rather large uncertainties, our simulation using the CLF in Figure 3 presumably provides a superior estimate of the population since more Centaurs are now known and a model of the distance distribution has been incorporated.

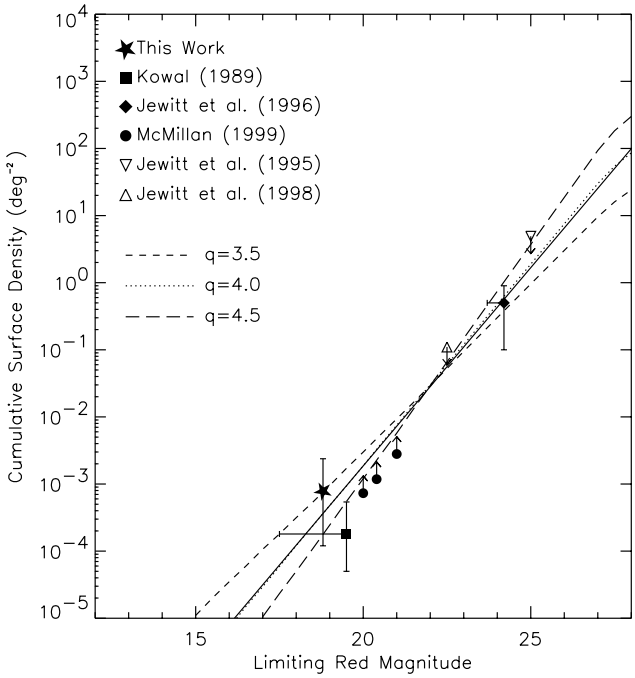

FIG. 4.—Simulations of the CLF of the Centaurs. This simulation used parameters $q = 3.5$, 4.0, and 4.5 with $r_{min} = 1$ km, $r_{max} = 1000$ km, $\gamma = -1.3$, $R_{min} = 10$ AU, and $R_{max} = 30$ AU. The solid line is the fit to the KBO data shifted vertically to fit the lower Centaur CLF. See the text for an explanation of the parameters.

Assuming that the Centaurs are supplied by the KBOs, in steady state we should have $N_C \sim N_K t_C/t_K$ where N_C is the number of Centaurs, N_K is the number of KBOs, t_C is the average Centaur lifetime, and t_K is the average KBO lifetime. For KBOs $t_K \approx 10^{10}$ yr (Quinn, Tremaine, & Duncan 1990), and for Centaurs $t_C \approx 10^6$–10^7 yr (Hahn & Bailey

TABLE 6

CENTAUR MONTE CARLO SIMULATION RESULTS

q[a]	γ[b]	Albedo	Γ	$N(r > 1)$[c]	$N(r > 50)$[c]	$N(r > 100)$[c]
3.0.....	−1.3	0.04	1.3×10^6	6.7×10^5	270	65
3.5.....	−1.3	0.04	7.5×10^6	3.0×10^6	170	30
4.0.....	−1.3	0.04	3.6×10^7	1.2×10^7	100	12
4.5.....	−1.3	0.04	1.8×10^8	5.0×10^7	60	5
4.0.....	−0.3	0.04	2.3×10^7	7.6×10^6	60	8
	−0.8	0.04	3.0×10^7	1.0×10^7	80	10
	−1.8	0.04	4.8×10^7	1.6×10^7	130	15
	−2.3	0.04	6.3×10^7	2.1×10^7	170	20
	−1.3	0.10	9.6×10^6	3.2×10^6	25	3
		0.40	1.2×10^6	3.9×10^5	3	0

[a] Index of power-law size distribution.
[b] Index of power-law distance distribution.
[c] Number of objects with radius greater than r in kilometers.

1990; Asher & Steel 1993; Levison & Duncan 1997). With $N_K \simeq 70{,}000$ ($r > 50$ km) KBOs (Jewitt et al. 1998), we expect $N_C \simeq 7$–70 ($r > 50$ km) Centaurs based on the steady state assumption. This is consistent with the $N_C \sim 100$ estimated here from the CLF, and consistent with the Kuiper Belt's supplying the Centaur population. Since the average Centaur lifetime expressed in years is similar to the number of Centaurs with radii greater than 1 km [$N(r > 1\ \mathrm{km})/t_C \sim 1$], about one Centaur with $r \geq 1$ km must be delivered to the gas giant region per year. Duncan, Levison, & Budd (1995) found the fraction of KBOs that leave the Kuiper Belt from planetary interactions to be 5×10^{-11} yr^{-1}. Assuming that half of the KBOs that leave the Kuiper Belt end up as Centaurs, then with 7×10^4 KBOs of $r > 50$ km and a Centaur lifetime of 10^6 to 10^7 yr we would expect between 2 and 20 Centaurs to be present with radii greater than 50 km, consistent with our results.

For a $q = 4$ size distribution, the total mass is

$$M = \frac{4 \times 10^9 \pi \rho \Gamma}{3} \left(\frac{0.04}{p_R}\right)^{3/2} \ln\left(\frac{r_{\max}}{r_{\min}}\right), \qquad (6)$$

where ρ (kg m^{-3}) is the bulk density. Using $\rho = 1000$ kg m^{-3} (similar to cometary nuclei), $p_R = 0.04$, $r_{\min} = 1$ km, and $r_{\max} = 200$ km (about the size of the largest known Centaur), we obtain $M \approx 8 \times 10^{20}$ kg ($\sim 10^{-4}\ M_\oplus$) for the current total mass of the Centaurs. Assuming that Centaurs have a lifetime of 5×10^6 yr and are in steady state, we find that 0.1 $M_\oplus$ has been cycled through the Centaurs during the 4.5×10^9 yr age of the solar system. If objects as large as Pluto ($r_{\max} = 1200$ km) with $\rho = 2000$ kg m^{-3} are considered, then the mass cycled through the Centaurs during the age of the solar system is about 2.5 times greater than the above result. Either way, it is comparable to the inferred total mass currently in the Kuiper Belt of $\sim 0.2\ M_\oplus$ (Jewitt et al. 1998).

Centaurs are close enough to the Sun to show cometary activity (e.g., Chiron), which can lead to an overestimate of their size if one assumes a constant albedo, as we have done. Observationally, most surveys are only sensitive to bright (large) Centaurs. Thus, the smaller Centaur population was obtained by extrapolating from larger Centaurs, which may not follow the same distribution. No survey has been specifically targeted at detecting Centaurs. Most surveys that have found Centaurs have been optimized instead for finding KBOs or asteroids. This makes it hard to assess the sensitivity to Centaurs of some published surveys. The surveys plotted in Figure 3 are those that were capable of finding Centaurs in at least the range of heliocentric distances 10 to 30 AU. Our survey was sensitive to Centaurs from 5 to 30 AU. Only four of the 20 currently known Centaurs could have radii greater than 50 km (assuming geometric albedo 0.04), and our simulation predicts ~ 100 such objects in the whole sky. Most would be located near but inside the orbit of Neptune, with apparent red magnitudes near 23. They would have naturally escaped detection in most wide-field surveys conducted to date.

3.2. *The Kuiper Belt*

Surface densities of KBOs from different surveys are in reasonable agreement for $20 \lesssim m_R \lesssim 26$ (Fig. 5). A weighted least-squares fit to the CLF for all the data with at least one detection is shown in Figure 5 (we used only the middle of the three Tombaugh points in the fit), yielding

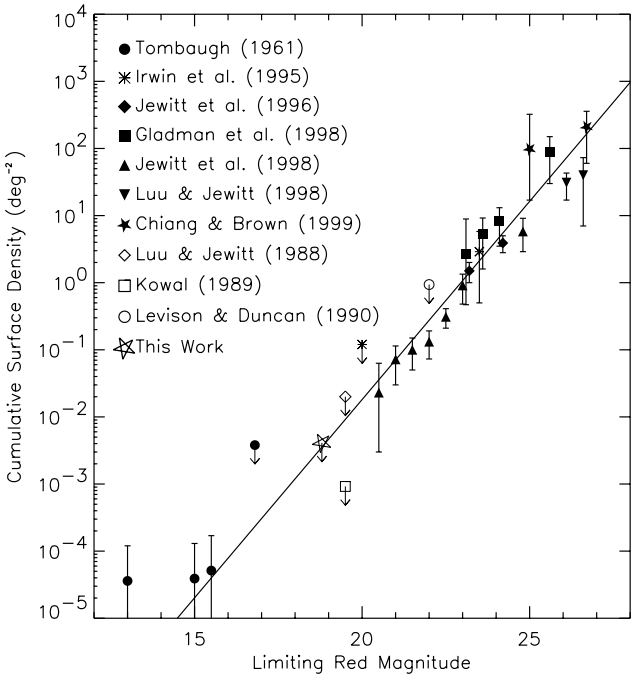

FIG. 5.—CLF of the Kuiper Belt. Symbols with arrows are 3 σ upper limits from surveys with null results. Other symbols are from various published surveys with 1 σ error bars. The solid line is the best fit to the data.

$\alpha = 0.59 \pm 0.05$, $m_0 = 23.0 \pm 0.2$. The fit is consistent with the fits found by Jewitt et al. (1998; $\alpha \simeq 0.55 \pm 0.05$, $m_0 \simeq 23.25 \pm 0.11$), Gladman et al. (1998; $\alpha = 0.76^{+0.1}_{-0.11}$, $m_0 = 23.40^{+0.20}_{-0.18}$), and Chiang & Brown (1999; $\alpha = 0.52 \pm 0.02$, $m_0 = 23.5 \pm 0.06$). Our survey's 3 σ upper limit is consistent with a constant slope for the CLF but does not rule out a steepening in the CLF for $m_R < 19$.

The above and some other previous works have improperly calculated the surface density from Tombaugh's (1961) survey (see Table 1 for the correct results). They used Tombaugh's follow-up survey, which was conducted to search for satellites or other objects that might be near Pluto. This survey reached $m_R = 16.8$ and covered 1530 deg^2 of sky. However, Pluto was discovered in a survey that reached only $m_R = 15.5$ and covered about 28,000 deg^2, initiated earlier and continued later (Table 1). The 1530 deg^2 survey should be interpreted as a null result since Pluto was not detected serendipitously. Therefore, the Tombaugh datum used in some earlier works should be shifted to brighter magnitudes and lower surface densities.

3.3. *Collision Clouds*

The Kuiper Belt was first thought to be collisionless, though it now appears that collisional effects might be very important (Davis & Farinella 1997). This has the result of removing the primitive and possibly unprocessed material from KBOs and might allow for dust to be observed in the Kuiper Belt. The collision products might be seen directly by the detection of dust clouds around the KBOs (C. Alcock & P. Hut 1993, unpublished; Stern 1996a). Assuming that there are 10^9 KBOs with $r > 1$ km and that the Kuiper Belt extends $\pm 30°$ from the ecliptic, Stern (1996a) and Alcock & Hut predicted between 1 and 100 collisions per year capable of producing detectable ($m_R \lesssim 15$) dust clouds.

The characteristic expansion time of a cloud is $t \approx r/v$, where v is the expansion velocity and r is the radius of the expanding cloud. The velocity of the ejected material depends on the energy of the impact and the sizes of the projectile and target. KBOs have Keplerian velocities of a few kilometers per second, and escape velocities for 1 km objects are around 1 m s^{-1}. The cloud should reach peak brightness in reflected light when its optical depth is unity. The time to reach peak brightness is $t \approx c/v$, where c is the critical radius at which optical depth unity is reached. The critical radius depends on the size distribution of ejected particles. If constant density is assumed, then the critical radius is just the square root of the geometric cross section of the particles [$c = a(a_i/a)^{1.5}$, where a is the average radius of particles created from the initial projectile radius of a_i]. The duration of visibility depends on the limiting magnitude. Using typical values of $v = 1$–5 km s^{-1} (the approximate expansion velocity of gas produced by impact vaporization) and a fixed size of 0.1 to 10 μm for particles in the cloud, we find that a dust cloud should reach optical depth unity in only a few days and be brighter than red magnitude 19 for about 20 to 100 days. If 100 clouds are produced in 1 year and each is visible for 50 days, about 14 clouds should be visible at any instant. With 14 clouds in 20,000 deg^2, we expect to find one cloud for every 1430 deg^2 of sky. Owing to the large pixels of the APT, our survey would not resolve one of these collision clouds if in our field of view, though we would detect the KBO-type movement of any clouds brighter than $m_R = 18.8$. No dust clouds brighter than $m_R = 18.8$ were detected in the 1428 deg^2 of sky searched in this survey. Assuming a Poisson spatial distribution, this yields a 3 σ confidence limit that there are fewer than 82 clouds for 20,000 deg^2 at any given time, or less than one cloud per 244 deg^2 of sky with $m_R < 18.8$. This also puts a 3 σ upper limit of 600 clouds produced per year with $m_R < 18.8$.

More sky must be searched to determine whether Pluto is just one of several other large KBOs waiting to be discovered. If the amount of sky searched for slow-moving objects were doubled, strong constraints on the bright end of the KBO CLF would be obtained. This survey was hindered by the large pixel size of the CCD. Currently, CCDs that are 4 times as large and with pixels half the size are routinely available. It is our goal to continue to survey the sky for bright SMOs with a larger CCD and smaller pixels. This will improve the efficiency of the survey and allow the data to be better sampled.

4. SUMMARY

1. A total of 1428 deg^2 of sky were searched for KBOs and Centaurs to a limiting magnitude of $m_R = 18.8$. One previously discovered Centaur was detected serendipitously (1997 CU_{26} [Chariklo]), and no KBOs were detected.

2. This survey, the largest published CCD survey to date sensitive to both Centaurs and Kuiper Belt objects, was analyzed both by an automated technique and by eye. The survey parameters were well established.

3. The cumulative surface density is $\Sigma_C = 7.8^{+16.0}_{-6.6} \times 10^{-4}$ deg^{-2} for Centaurs at $m_R = 18.8$, with error bars at the 1 σ level. The Centaur cumulative luminosity function has a slope ($\alpha \sim 0.6$) similar to the Kuiper Belt CLF but shifted about 1.5 mag fainter. The number of Centaurs per unit sky area is about 1/10 the number of KBOs at any given magnitude.

4. A Monte Carlo simulation was performed to obtain the expected number distribution of Centaurs. Differential power-law size distribution indices between $q = 3.5$ and $q = 4.5$ are consistent with the Centaur CLF. Using $q = 4$, we find that there are about 1×10^7 Centaurs with radii larger than 1 km, and $\sim$100 larger than 50 km in radius, of which only four (Chiron, Pholus, Chariklo, and 1995 DW_2) are presently known. The combined mass of all Centaurs is 10^{-4} $M_\oplus$. Assuming a steady state, this implies that 0.1 $M_\oplus$ has been cycled from the Kuiper Belt through the Centaurs during the age of the solar system.

5. The surface density of Kuiper Belt objects at $m_R = 18.8$ is $\Sigma_K < 4.1 \times 10^{-3}$ deg^{-2} at the 3 σ confidence level. This result is consistent with the previously determined CLF for Kuiper Belt objects but does not rule out a steepening in the slope for $m_R < 19$.

6. No collisionally produced dust clouds were observed in the Kuiper Belt. We place a 3 σ upper limit of 600 visible collisional clouds ($m_R < 18.8$) produced per year.

We thank Jill Rathborne for observational assistance, and Robert McMillan, Jeff Larsen, Bruce Koehn, and Steve Larson for very helpful information about their near-Earth object surveys. This work was supported by a grant to D. C. J. from NASA.

REFERENCES

Asher, D. J., & Steel, D. I. 1993, MNRAS, 263, 179
Carter, B. D., Ashley, M. C. B., Sun, Y.-S., & Storey, J. W. V. 1992, Proc. Astron. Soc. Australia, 10, 74
Chiang, E. I., & Brown, M. E. 1999, AJ, 118, 1411
Davis, D. R., & Farinella, P. 1997, Icarus, 125, 50
Duncan, M. J., Levison, H. F., & Budd, S. M. 1995, AJ, 110, 3073
Gehrels, N. 1986, ApJ, 303, 336
Gladman, B., Kavelaars, J. J., Nicholson, P. D., Loredo, T. J., & Burns, J. A. 1998, AJ, 116, 2042
Hahn, G., & Bailey, M. E. 1990, Nature, 348, 132
Irwin, M., Tremaine, S., & Żytkow, A. N. 1995, AJ, 110, 3082
Jedicke, R., & Herron, J. D. 1997, Icarus, 127, 494
Jewitt, D., Luu, J., & Chen, J. 1996, AJ, 112, 1225
Jewitt, D., Luu, J., & Trujillo, C. 1998, AJ, 115, 2125
Jewitt, D. C., & Luu, J. X. 1995, AJ, 109, 1867
Kenyon, S. J., & Luu, J. X. 1999, ApJ, 526, 465
Kowal, C. T. 1989, Icarus, 77, 118
Landolt, A. U. 1992, AJ, 104, 340
Levison, H. F., & Duncan, M. J. 1990, AJ, 100, 1669
———. 1997, Icarus, 127, 13
Luu, J. X., & Jewitt, D. 1988, AJ, 95, 1256
Luu, J. X., & Jewitt, D. C. 1998, ApJ, 502, L91
Moffat, A. F. J. 1969, A&A, 3, 455
Morbidelli, A., & Valsecchi, G. B. 1997, Icarus, 128, 464
Quinn, T., Tremaine, S., & Duncan, M. 1990, ApJ, 355, 667
Singer, S. F. 1975, Icarus, 25, 484
Stern, S. A. 1996a, A&A, 310, 999
———. 1996b, AJ, 112, 1203
Tedesco, E. F. 1989, in Asteriods II, ed. R. Binzel, T. Gehrels, & M. Matthews (Tucson: Univ. Arizona Press), 1090
Tombaugh, C. 1961, in Planets and Satellites, ed. G. P. Kuiper & B. M. Middlehurst (Chicago: Univ. Chicago Press), 12
Trujillo, C., & Jewitt, D. 1998, AJ, 115, 1680